

# Low AC Resistance Foil Inductor

West Coast Magnetics

## I. Introduction

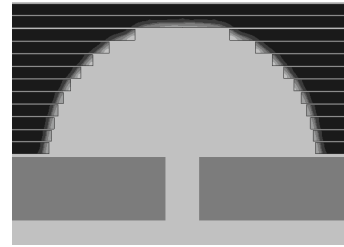
Electrical energy is rarely supplied in the form it is needed. The process of power conversion is used in an extremely large number of devices that perform a wide variety of functions. Power electronics has seen advances in the past several decades that have allowed for countless new applications and have vastly improved the efficiency of current power-conversion circuitry. The potential annual energy savings has been estimated at \$200 billion, considering only lighting, motor, and automotive applications. The magnetics of power electronics has particular potential for improvement, as these components are typically the largest, most expensive, and volumetrically inefficient in a power circuit. Existing magnetic components are many times the greatest source of power loss and the biggest barrier to performance increases and size reduction.

There are two principle mechanisms for loss in magnetic components, core losses and winding losses. Core losses involve the magnetic properties of the core material, which exhibits power losses in the form of hysteresis and eddy currents within the core itself. The core material must be chosen with a permeability and saturation flux density appropriate to the application to minimize these energy losses. Winding losses come from the resistance in the conductive material. This loss has both dc and ac components. The dc component is proportional to the length and inversely proportional to the cross-sectional area of wire used. If the device is carrying a current with an ac component, there are also losses due to eddy currents and the proximity effect if multiple turns are used. A time-dependent current induces a flux, which in turn induces small currents within the wire. The result is a current density profile concentrated on the surface of the

conductor at a distance of a skin depth, defined as  $\delta = \sqrt{\frac{\rho}{\pi \cdot \mu \cdot f}}$ , where  $\mu$  is the

permeability,  $\rho$  the resistivity, and  $f$  the frequency. Since very little current passes through the center of the winding, the effective cross-sectional area is reduced and the resistance is increased. These losses increase in magnitude as the frequency and current increase. Power loss in any magnetic device is the sum of these effects, and the design process is made more difficult by their relationship to one another. For instance, common methods of reducing ac resistance, such as the use of litz-wire, greatly reduce the cross-sectional area of the conductor and drastically increase dc resistance. Foil inductors are often used to minimize winding losses in an application of high dc current because of their efficient use of the winding window. However even a small amount of ac current can cause significant losses in these coils. Such sacrifices are unacceptable in many of today's applications. Many dc-dc converters require an inductor that can carry a large dc current with an ac ripple. Even when the ac component is small in comparison to the dc current, the ac resistance can be orders of magnitude larger the dc resistance.

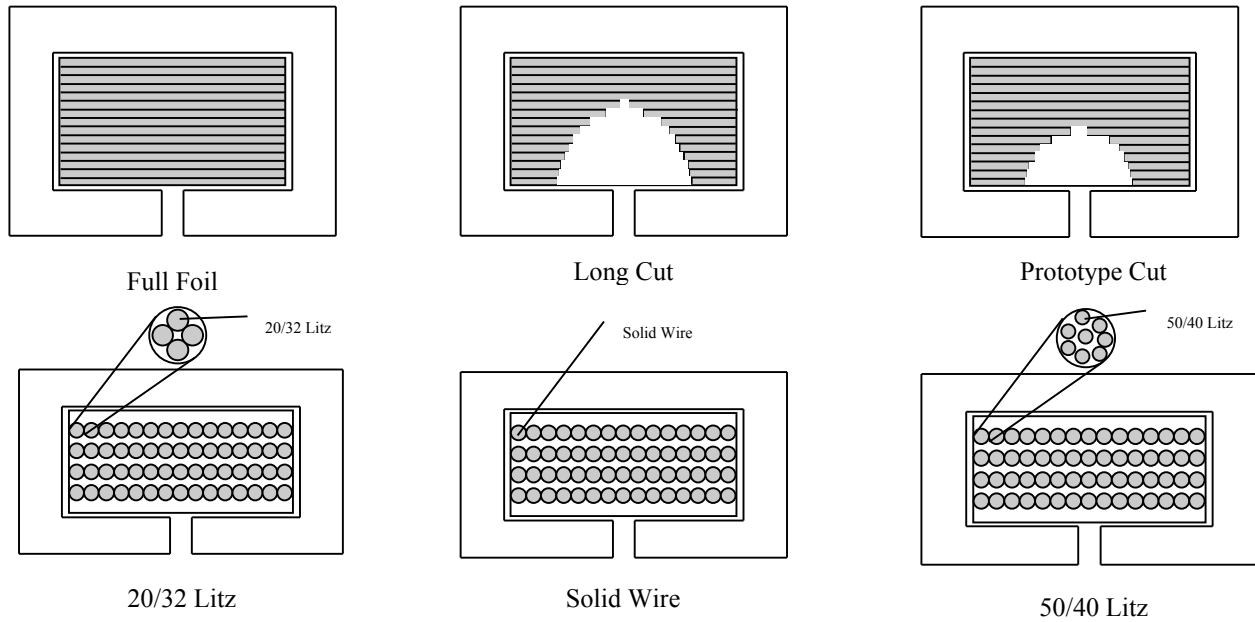
West Coast Magnetics, in collaboration with Thayer School of Engineering at Dartmouth College, is investigating different winding geometries that significantly reduce ac resistance in gapped foil inductors with only a small increase in dc resistance. The conventional foil winding is modified by removing the copper in the vicinity of the air gap in the core, preventing the fringing flux of the gap to affect the current within the conductor. The current distribution can then be concentrated around the gap, as shown on the right, with a higher current density shown in lighter grey. The slightly smaller cross-section of the copper increases the dc resistance by a small amount, however ac resistance is lowered and the overall performance is improved. A program has been authored to optimize the size and shapes of such windings based on the current present, and accurately predict their performance. Much has already been written on the optimization and prediction methods of the software, and will consequently not be discussed in detail here (see Pollock and Sullivan, "Modeling Foil Winding Configurations With Low AC and DC Resistance" for more information).



## II. Scope Of Study and Inductor Design

West Coast Magnetics and Dartmouth College have compared this new technology to conventional winding types through experimentation. The purpose of this work is to confirm that the foil technology is superior to conventional winding types, and to verify that the inductor temperature rise under load is as expected. The present work does not explore optimal foil designs, or compare methods of measuring and simulating losses, as Jenna Pollock and Charlie Sullivan at Thayer School have already completed this work. The inductors were constructed around an E70/33/32 ferrite core of material EPCOS N67 and gapped 2.63 mm in the center leg (designated B66371-G-X167). Each half was gapped 1.32 mm to insure that the gap was centered. Fifteen turns were wound on a rectangular bobbin, producing an inductance of 90-95  $\mu\text{H}$ . Six different winding options were chosen for comparison based on current practices. In every case, the conductor area was maximized in the winding window. In the case that wire was used, the 15 turns were wound on the same layer, then additional layers were wired in parallel to fill the window. A standard foil inductor was constructed of 15 turns of 0.020" copper, measuring 1.55" in width and separated by .003"x1.69" Nomex. Five prototype coils were built using the new technology optimized for a current of 40 A dc with a 15% (6 A peak-to-peak) ripple at 50kHz. The construction of these coils was similar; however, a semicircular gap with a radius of 7.1 mm was left in the conductor around the air gap in the core. An additional inductor utilizing the new technology was also constructed, optimized for a ripple of 22.5% at 50 kHz and with a larger portion of conductor removed. Several wire inductors were also built for comparison, one of solid-wire and two consisting of litz-wire of various stranding. The solid-wire winding consisted of four layers in parallel of 15 turns of solid-wire. Two litz-wire coils were constructed based on litz-wire gauges commonly used at the test frequency of 50kHz. The first stranding was four twisted strands of 20/32 litz, the second consisted of 8 twisted strands of 50/40 litz. These configurations were

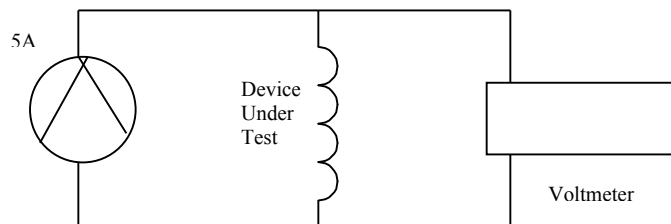
each wound in 4 parallel layers of 15 turns. Cross sections of the winding windows are shown below.



### III. Estimate of Power Loss

In order to determine and compare the performance of the inductors, the dc resistance and ac resistance were measured and this data was then used to determine a theoretical power loss for each coil. The dc resistance was determined by measuring the voltage drop across the coil carrying a 5 A current. The resistance was then calculated using Ohm's law,  $V = I \cdot R$ . The test circuit is and results are shown below. The power loss from the 40A dc current can be found using the equation  $P = I^2 R$ .

Coil	Vdc (mV)	Rdc (Ohm)
Prototype 1	11.58	0.002316
Prototype 2	11.44	0.002288
Prototype 3	11.04	0.002208
Prototype 4	11.05	0.00221
Prototype 5	11.09	0.002218
Full Foil	10.64	0.002128
Long Cut	12.31	0.002462
20/32 Litz	19.22	0.003844
50/40 Litz	26.86	0.005372
Solid-wire	13.06	0.002612

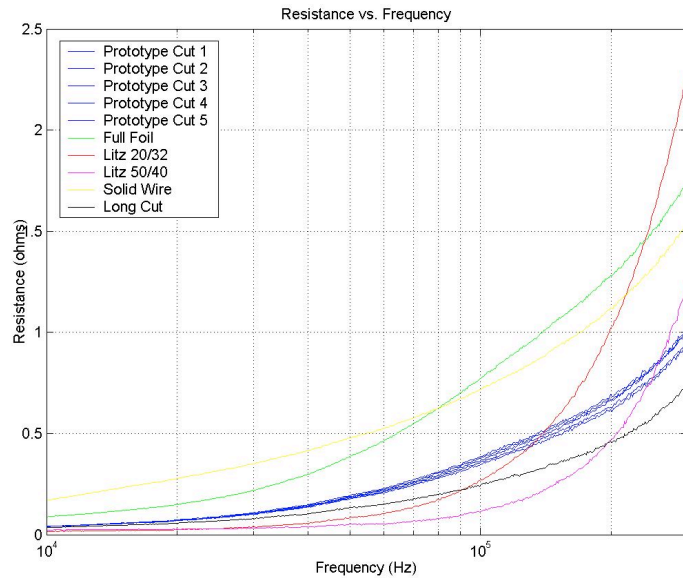


A measure of the ac resistance was obtained by sweeping each coil with an Agilent 4294A Precision Impedance Analyzer from 1 kHz to 1MHz. The result is a resistance at

Frequency (Hz)	Fourier Coefficient
50000	0.5732
150000	0.0637
250000	0.0229
350000	0.0117
450000	0.0071
550000	0.0047
650000	0.0034
750000	0.0025
850000	0.0020
950000	0.0016

equation  $P = I_{rms}^2 R$  was then used along with the impedance analyzer data at each of the frequencies to the left and summed to find the total ac power loss for each coil. A larger or smaller ripple ratio affects only the magnitude of the Fourier coefficients and thus rms current amplitude, and the losses are similarly straightforward to calculate.

each sinusoidal frequency in the above range. The portion of the result between 10 kHz and 200 kHz is shown in the chart below. The current in the test case however is a 6 A triangular ripple superimposed on a 40 A dc current. Fourier decomposition was performed on the triangle wave so that the sinusoidal data from the Agilent 4294A could be used to estimate the resistance of the inductors to a triangle wave. The frequencies present and their Fourier coefficients are shown in the table. The power loss



Core losses are very small in magnitude compared to winding losses but should still be accounted for. Since core losses depend only on the core material, ripple current, inductance, and core geometry, and because they are small compared to winding losses, they are considered to be the same for all coils. There were calculated using the equation below, where  $B_{pk}$  is the peak AC flux density (in gauss),  $\Delta I$  is the peak to peak ripple current,  $L$  is the inductance,  $A$  is the cross-sectional area, and  $N$  is the number of turns. The data for the equation is taken from the core data sheet.

$$B_{pk} = \frac{L \cdot \Delta I \cdot 10^8}{2 \cdot A \cdot N}$$

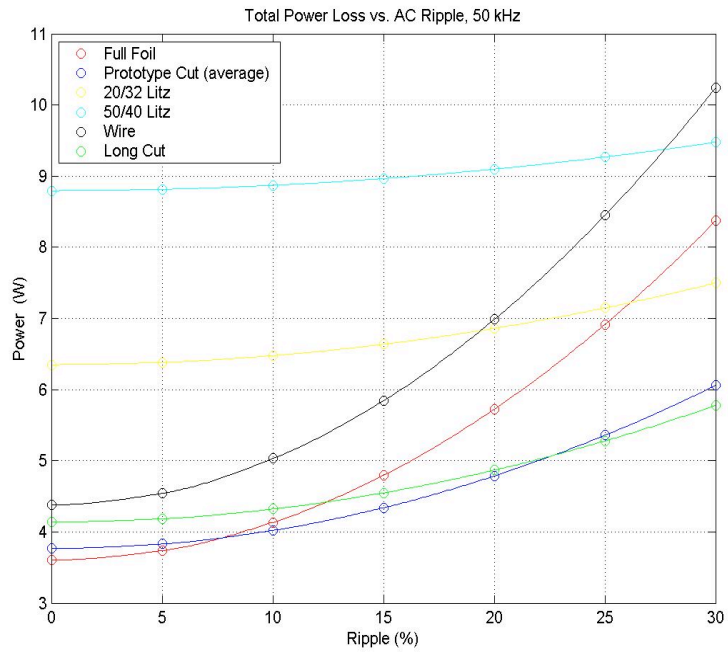
$L$	$9.0 \times 10^{-5} \text{ H}$
$\Delta I$	$6 \text{ A}$
$A$	$6.83 \text{ cm}^2$
$N$	$15$

The calculated peak flux density of 263 Gauss corresponds to a power loss of approximately 0.2 W for the core volume of  $103 \text{ cm}^3$  at 20 degrees C.

The total power loss of each coil was calculated by adding together the ac power loss, the dc power loss, and the core losses. The results are shown in the chart and summarized at the optimized ripple ratio below.

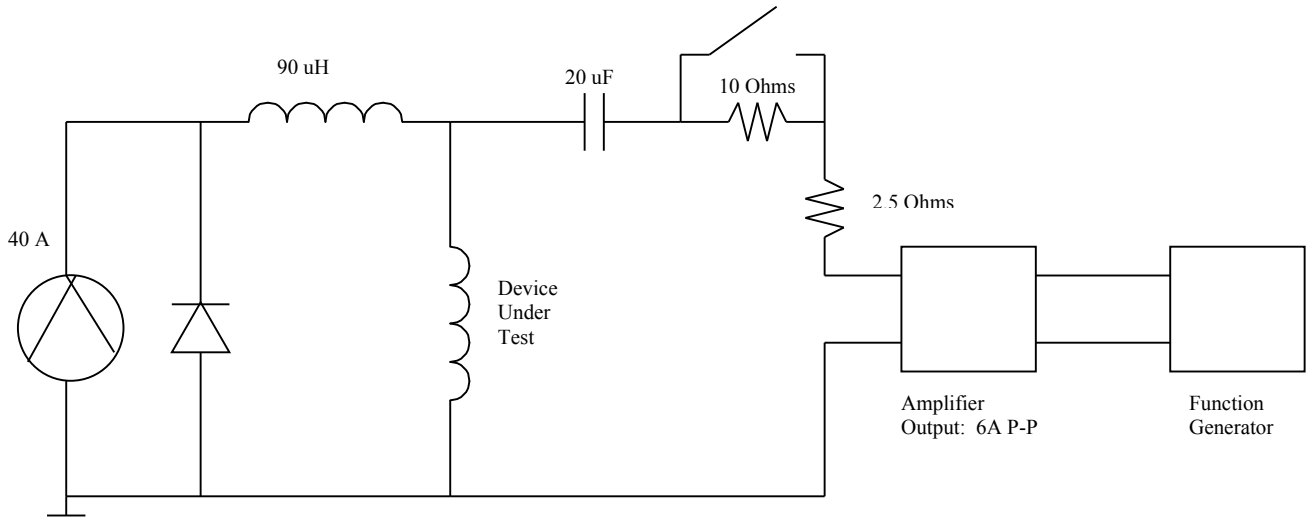
Coil	Power (W)
Prototype (average)	4.3099
Full Foil	4.7962
Long Cut	4.5493
20/32 Litz	6.6374
50/40 Litz	8.9657
Solid-wire	5.8445

The prototype has a power loss that is approximately 0.5 watts lower than the full foil winding, a 10.58% increase in efficiency. Larger ripple ratios favor the new technology much more, and show a more drastic increase in performance. Also at higher ripples the larger cut becomes more efficient than the 5 prototypes, consistent with the fact that the fringing flux is greater in these cases as well.



#### IV. Testing of Inductors Under Load

To experimentally confirm that the inductors perform as expected, we measured the temperature rise of the coils in a test circuit under the design conditions for this inductor. The test circuit was developed to load the inductor with the design conditions of 40 A dc with a 6 App ripple at 50 kHz. Each inductor was separately loaded in this circuit and



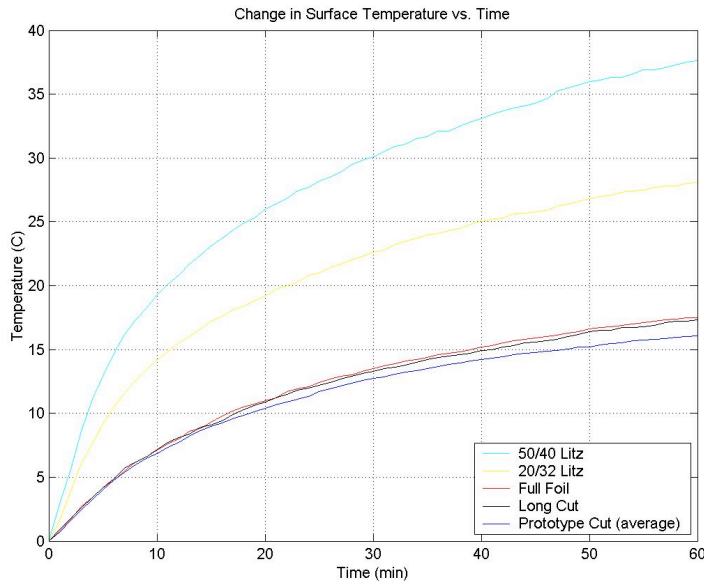
thermal measurements were made on the surface of the coils in order to verify that temperature rise correlated with the loss calculations above. The thermal resistance of the B66371-G-X167 core taken from the core data sheet is 5.5 K/W, and the predicted

steady state temperature changes are shown in the table below. The coils were placed in the circuit shown and subject to the test conditions for 60 minutes, with the surface

Coil	Predicted Temperature Rise (K,C)
Prototype (average)	23.7
Full Foil	26.4
Long Cut	25.0
20/32 Litz	36.5
50/40 Litz	49.3
Solid-wire	32.1

temperature taken every minute. Thermocouples were also placed between the first and second turn and before the last turn to monitor hot spot temperature, however this data will not be shown (See Appendix 1). The results are consistent with the power loss data calculated from the ac and dc resistances. The actual temperature

rises are recorded in the table.



Coil	Actual Temperature Change (C) after 60 min
Prototype (average)	16.05
Full Foil	17.5
Long Cut	17.3
20/32 Litz	28.1
50/40 Litz	37.6
Solid-wire	---

The duration of the test was not sufficient to reach steady-state temperatures; however there is enough data for the behavior of the coils to be inferred. The wire coil was not available for test at the time of the experiment, yet there is no reason to believe its performance would not correlate to the power loss data as the other inductors do. There is a temperature difference of 1.45 degrees C after 60 minutes, compared to the predicted 2.67 degrees.

The discrepancy can be attributed to the experiment not running long enough to reach steady state, where the temperature difference would likely be much closer to the predicted value. Regardless, the new technology brings a clear improvement over the alternative windings.

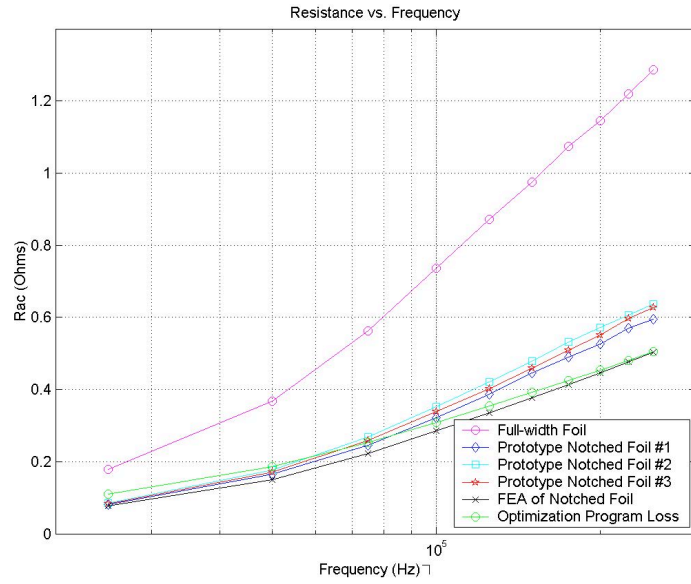
#### IV. Accuracy of Model

Another very interesting comparison is between the actual and predicted performance of the coils. Shown is the ac resistance of three of the prototype coils, the results of the finite element analysis (FEA) simulations, and the predicted value from the optimization program. The theoretical results are slightly lower, as they don't take into account errors in the winding or cutting of the foil, inaccuracies that would cause an inductor to perform less than ideally. In each case the differences are on the magnitude of tenths or even

hundredths of an ohm. The performance of a full foil winding is shown as a reference. This places tremendous confidence in the ability of the software to both correctly optimize a coil for a given scenario and accurately predict its performance.

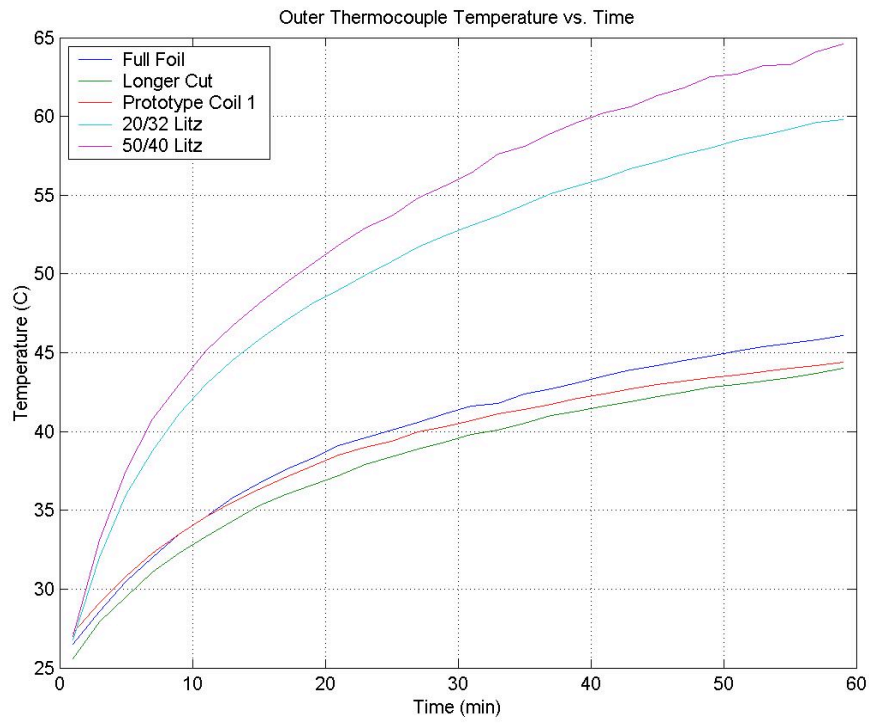
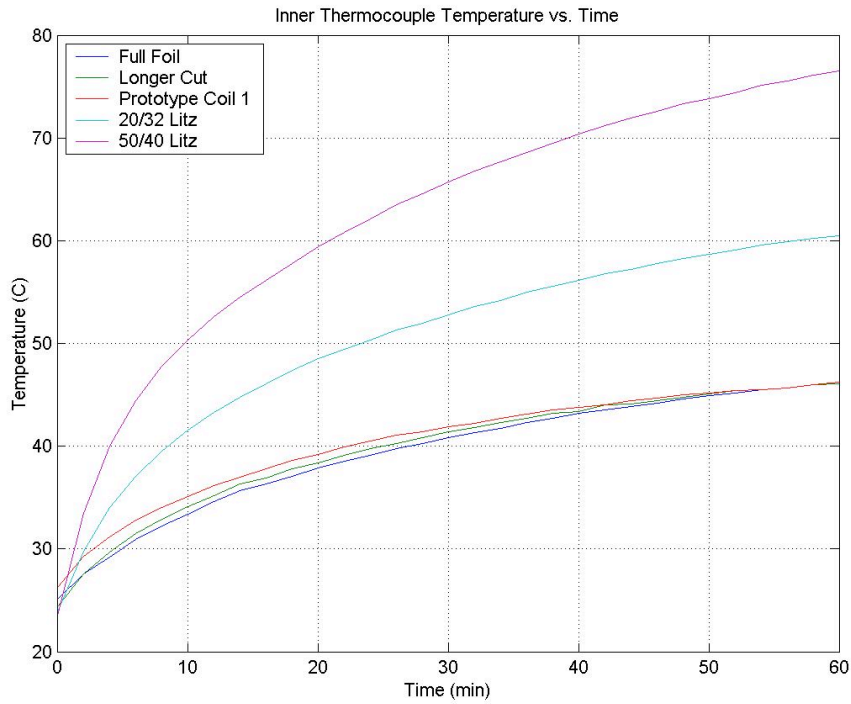
## VI. Conclusion

This study unequivocally shows that the technology developed by West Coast Magnetics and Dartmouth College offers a marked improvement over standard inductor winding techniques, including litz-wire and conventional foil windings. The new coils display a lower ac resistance, power loss, and surface temperature rise than all design alternatives in this study. In addition to displaying approximately a 10% increase in performance, a number that will only increase with the amount of current and ripple present, the conducted experiments confirm the accuracy of the design program. It is thus possible to find the best geometry and build an optimal inductor for many scenarios with a high degree of confidence.



# Appendix 1

## Inner and Outer Thermocouple Temperatures



## Appendix 2 AC Resistance and Total Power Loss (at 50 kHz)

